Superfluorescent erbium doped fibre optic sources comparative study

M. A. Quintela*, C. Lavin, M. Lomer, A. Quintela, J. M. López-Higuera
Photonics Engineering Group, Dpto. TEISA, ETSIIT – University of Cantabria,
Avda. los Castros s/n, cp. 39005, Santander, Spain

ABSTRACT

The theoretical design and experimental characterization of 1480 nm superfluorescent erbium-doped fibre sources are reported in this paper. Different configurations and three erbium doped fibres with different concentrations are used. In double pass configurations a Faraday rotator mirror is used. The comparison of the characteristics of these SFSs in terms of the output power, mean wavelength, spectral width and stability is carried out.

Keywords: amplified spontaneous emission, broadband light source, erbium doped fiber, Fararday rotator mirror.

1. INTRODUCTION

The amplified spontaneous emission (ASE) of the erbium doped fibre (EDF) is considered in the most case an undesired effect because it contributes to the degradation of the performance of the erbium doped amplifier and fibre laser. Nevertheless, this kind of emission presents some characteristics that permit the design and develop of low-coherence EDF source (superfluorescent erbium doped fibre). The characteristics of these sources are: high efficiency, high spatial coherence, broad spectral emission, and high stability of the mean wavelength. Erbium-doped superfluorescent fibre source (SFS) are very useful for various areas, such as sensing, for optical device testing and in a wide range of applications including white light optical interferometric based devices and fibre optic gyroscopes [1].

In this paper the theoretical model of SFS sources is presented. Three erbium-doped fibres with different concentrations have been used. To check the simulation results, experimental works were realized for three erbium-doped fibres pumped at 1480 nm and in several different configurations. The election of this pump wavelength is due to the quantum conversion efficiency of 1550 nm ASE with the pump wavelength of 1480 nm is higher than that with 980 nm pump wavelength [2].

Although in almost all the works presented by others authors typical mirrors are used in a double pass configuration, in this paper a Faraday rotator mirror (FRM) has been used instead of a mirror. The FRM reduces the output mean wavelength polarization dependence [3], [4]. Furthermore, the broadband of the FRM reflectivity permits that the pumping signal is also reflected by the FRM and, as a consequence, the efficiency improves.

The structure of the paper is as follows, in section 2, the basic theory of SFSs, different configurations and simulation considerations are described. In section 3 simulation results are presented. The next section presents the experimental results and their discussion. Finally, several conclusions are extracted.

2. THEORY OF THE BROADBAND ERBIUM-DOPED SUPERFLORESCENT FIBER SOURCE

2.1 Output parameters

The output signal of the SFS is defined by the output spectral power in a range of optical frequencies ($P(\lambda)$). The parameters more important and representative of this source can be obtained from this function. The total output power is calculated from the integration of $P(\lambda)$:

$$P_o = \int P(\lambda) d\lambda \tag{1}$$

*quintelm@unican.es; phone +34 942 200877 Ext. 18; fax+34 942 200877; grupos.unican.es/gif/

Optical Fibers: Applications, edited by Leszek R. Jaroszewicz, Brian Culshaw, Anna Grazia Mignani
Proc. of SPIE Vol. 5952, 59521P, (2005) · 0277-786X/05/$15 · doi: 10.1117/12.623183

The mean wavelength ($\bar{\lambda}$) and the spectral width ($\Delta\lambda$) are other important parameters of SFSs. They are defined as follows [1]:

$$\bar{\lambda} = \frac{\sum P(\lambda_i)\cdot\lambda_i}{\sum P(\lambda_i)} \tag{2}$$

$$\Delta\lambda = \frac{\left[\sum P(\lambda_i)\Delta\lambda_i\right]^2}{\sum P^2(\lambda_i)\Delta\lambda_i} \tag{3}$$

where λ_i is the wavelength of ith ASE wave and $\Delta\lambda_i$ is the spectral width by ith ASE wave.

The spectral width provides information about the relation between the two principal spectral bands of the EDF (1532 nm and 1558 nm, respectively). On the other hand, the mean wavelength is temperature dependent and this can be represented by:

$$d\bar{\lambda}/dT = \left[\delta\bar{\lambda}/\delta T\right] + \left[(\delta\bar{\lambda}/\delta P_{bombeo})\cdot(\delta P_{bombeo}/\delta T)\right] + \left[(\delta\bar{\lambda}/\delta\lambda_{bombeo})\cdot(\delta\lambda_{bombeo}/\delta T)\right] \tag{4}$$

Where the first term is due to intrinsic thermal effects of the EDF, which typical values are minor that 10 ppm/°C [5]. The second and third terms represent the mean wavelength variation with pump power and pump wavelength, respectively. It is always desirable to have temperature independent ($d\bar{\lambda}/dT \cong 0$). The $\delta P_{bombeo}/\delta T$ and $\delta\lambda_{bombeo}/\delta T$ in the second and third terms depend on the characteristics of the pump source. Nevertheless, the $\delta\bar{\lambda}/\delta P_{bombeo}$ and the $\delta\bar{\lambda}/\delta\lambda_{bombeo}$ can be reduced by optimizing the SFS design parameters (EDF length, pump power and mirror reflectances) and by operating the pump wavelength closer to its peak absorption wavelength.

2.2 Theoretical model

To obtain the equations that define the behaviour of the SFS sources, the ASE spectrum is divided in n regions, each one with an optical frequency $\upsilon_{s,i}$ and a fix spectral width $\Delta\upsilon_h$. Therefore, tree signal powers are defined in each region: forward ASE ($P_s^+(z,\upsilon_{s,i})$), backward ASE ($P_s^-(z,\upsilon_{s,i})$) and pump signal ($P_b(z,\upsilon_p)$). When the pump wavelength is 1480 nm, these powers can be described from the following expressions:

$$\frac{dP_s^{\pm}(z,\upsilon_s,i)}{dz} = \pm\left[\gamma_s(z,\upsilon_s,i)P_s^{\pm}(z,\upsilon_s,i) + \gamma_{es}(z,\upsilon_s,i)2h\upsilon_{s,i}\frac{(\Delta\upsilon_h)}{n}\right] \tag{5}$$

$$\frac{dP_b(z,\upsilon_b)}{dz} = -\left[\gamma_b(z,\upsilon_b)P_b(z,\upsilon_b)\right] \tag{6}$$

with

$$\gamma_s(z,\upsilon_s,i) = \Gamma_s\left[\sigma_e(\upsilon_s,i)N_u(z) - \sigma_a(\upsilon_s,i)N_l(z)\right]$$

(7)

$$\gamma_{es}(z,\upsilon_s,i) = \Gamma_s\left[\sigma_e(\upsilon_s,i)N_u(z)\right] \tag{8}$$

$$\gamma_b = \Gamma_b\left[\sigma_{ab}(\upsilon_b)N_l(z) - \sigma_{eb}(\upsilon_b)N_u(z)\right] \tag{9}$$

N_u y N_l are defined as the population density of Er^{+3} ions (ions/m^3), in the excited state ($^4I_{13/2}$) and the fundamental state ($^4I_{15/2}$), respectively [6].

$$N_u(z) = \frac{N_T\left[\alpha W_s(z) + W_b(z)\right]}{(1+\alpha)W_s(z) + (1+\frac{1}{\beta})W_p(z) + \frac{1}{\tau_{21}}} \tag{10}$$

$$N_l(z) = N_T - N_u(z) \tag{11}$$

where N_T is the total population density of Er^{+3} ions, τ_{21} is the fluorescence time. W_s is the stimulated emission rate and W_b is the pump rate, and they are defined as:

$$W_s(z) = \frac{\Gamma_s\sigma_{es}}{h\nu A}\left[P_s^+(z) + P_s^-(z)\right] \tag{12}$$

$$W_b(z) = \frac{\Gamma_b\sigma_{es}}{h\nu_b A}\left[P_b(z)\right] \tag{13}$$

where υ is the frequency of each signal of the ASE spectrum, υ_p is the frequency of the pump signal, h is the Planck constant, A is the core area of the EDF, Γ_S and Γ_b are the overlap factor of the ASE signal and the pump signal, respectively.

The parameters α and β are the relation between the absorption cross section and emission cross section for the signal ASE and the pump signal, respectively.

$$\alpha = \frac{\sigma_{as}}{\sigma_{es}} \tag{14}$$

$$\beta = \frac{\sigma_{ab}}{\sigma_{eb}} \tag{15}$$

where σ_{as} and σ_{ab} are the absorption cross section of the ASE signal and the pump signal, respectively, and σ_{es} and σ_{eb} are the emission cross section of the ASE signal and the pump wavelength, respectively.

In this theoretical model, the ASE spectrum is divided in 10 regions (n=10) with $\Delta\nu_h$=4 nm. As a consequence, a differential equations system of 21 equations must be solved to obtain the values of the output signal power as a function of the design parameters.

The definition of contour conditions according to the SFS configuration is the last pass to solve this system. Four basic configurations can be defined depending on the direction of the output light and the mirror reflectances. These configurations are represented in fig. 1. As can be shown in this figure, two wavelength multiplexers (WDM) are used to separate the ASE signal and the pump signal. The mirror reflectances are represented by the transmittance T_1 and T_2. Contour conditions, the WDM whereby the output signal exit and the value of the transmittance in each FDE extreme are shown in table 1.

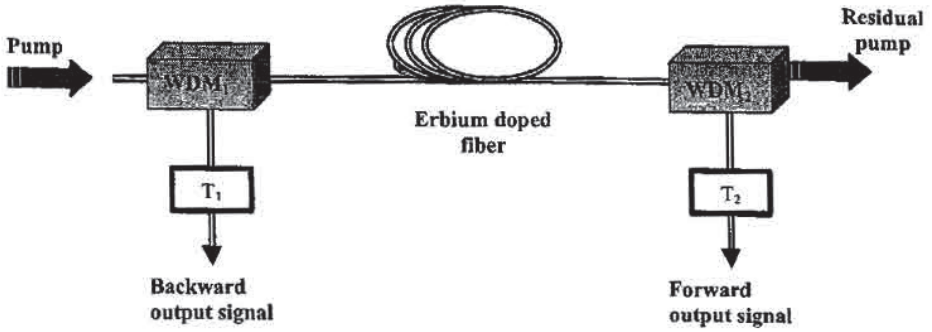

Figure 1. Configurations of the SFS sources.

CONFIGURATION	OUTPUT	T_1	T_2	CONTOUR CONDITION IN $z=0$	CONTOUR CONDITION IN $z=L$
SPF	WDM_2	1	1	$P^+(z=0)=0$	$P^-(z=L)=0$
SPB	WDM_1	1	1	$P^-(z=0)=0$	$P^+(z=L)=0$
DPF	WDM_2	0	1	$P^+(z=0)=R_1P^-(z=0)$	$P^-(z=L)=0$
DPB	WDM_1	1	0	$P^-(z=0)=0$	$P^+(z=L)=R_2P^-(z=L)$

Table 1. Contour conditions for different SFS configurations. (SPF: single pass forward, SPB: single pass backward, DPF: double pass forward, DPB: double pass backward).

3. SIMULATION RESULTS

The starting point of the design of the SFS sources is the choosing of the type of configuration and the EDF length. In this work, tree different EDFs have been used to design which properties are shown in table 2. The commercial fibre is a typical EDF and LRL and LSL fibres are high concentration EDFs of OFS.

	Commercial fibre	Fibra LRL	Fibra LSL
Absorption peak (≈1530 nm)	4,366 dB/m	24,76 dB/m	16,82 dB/m
Absorption peak (≈1480 nm)	1,21 dB/m	6,86 dB/m	4,5 dB/m
Er+3 concentration	$0,5\cdot10^{25}$ m^{-3}	$3,07\cdot10^{25}$ m^{-3}	$1,29\cdot10^{25}$ m^{-3}
Numeric aperture	0,1584	0,257	0,26
Core radio	2,644 μm	1,89 μm	1,76 μm

Table 2. EDF characteristics

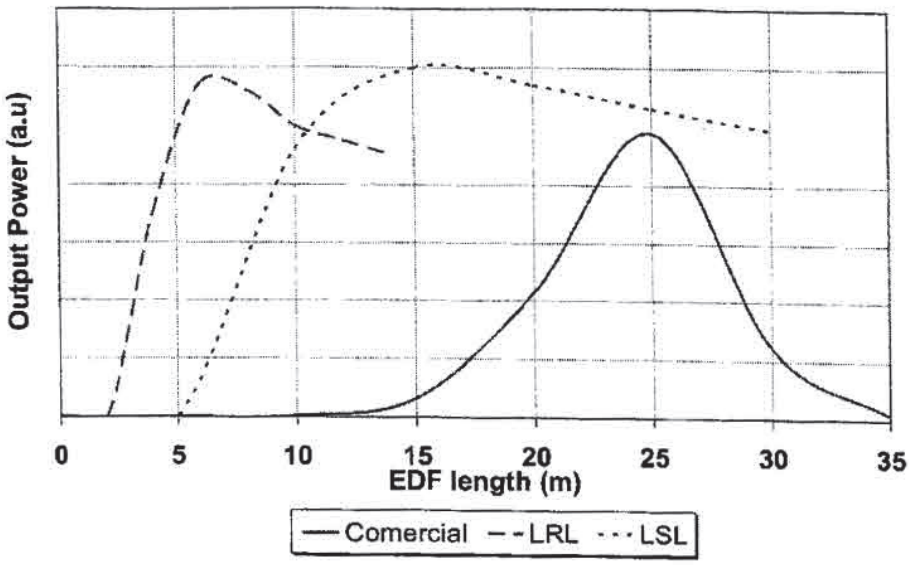

Figure 2. Simulation Results of the optimum length.

The output power of different SFS configurations as a function of EDF length for these tree fibres has been simulated. The results of DPB configuration are shown in fig. 2. From the figure, it can be deduced that the optimum length to maximum output power is inversely proportional to ion Er^{+3} concentration. The commercial, LRL and LSL EDF have an optimum length of 24-25 meters, 15-16 meters and 6-7 meters, respectively. On the other hand, the efficiency of the source isn't related with Er^{+3} concentration. The LSL is the fibre that permits obtain the maximum power with an adequate fiber length. This result will be experimentally checked.

4. EXPERIMENTAL RESULTS

Some works of others authors present the DPB configuration as the optimum configuration from the point of view of wavelength stability, spectral width and output power is the DPB [5],[7],[8] when the pump wavelength is 980 nm. Nevertheless, in this work the study of others configurations have been considered because they can introduce advantages with respect to the DPB configuration when the pump wavelength is 1480 nm. The general set-up shown in fig. 1 was used to experimentally characterize the SFS sources. An isolator at the source output is additionally used to prevent lasing in the presence of external feedback. The EDF was pumped by a 1480 nm pump laser diode (FOL1405RTD) with a maximum power of 300 mW. In the double-pass sources, a Faraday rotator mirror (FRM) ISOWAVE made of YIG material was used.

The output spectrum of the SPB and DPB configurations for the commercial EDF and different pump powers are shown in fig. 3(a) and fig. 3(b), respectively. As can be observed, the SPB configuration has a spectrum flatter than the DPB configuration (the relative power of two peaks of ASE spectrum (1532 nm and 1558 nm) is similar in the SPB configuration). This means that the spectral width of this configuration is bigger. The difference of spectral width between the configuration SPB and DPB for both LRL and LSL fibres is not so large.

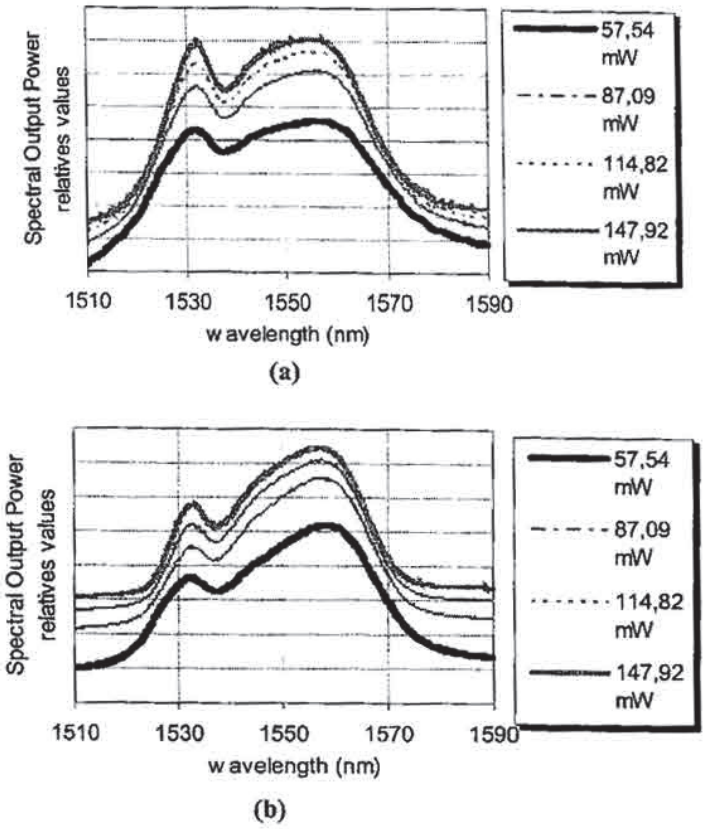

Figure 3. Evolution of the output spectrum with the pump power for the commercial EDF a) SPB configuration; b) DPB configuration.

The output spectrums of the DPF configuration for the commercial and LRL EDF are shown in figure 4(a) and 4(b), respectively. As can be seen in these graphs, the shape of ASE spectrum is different depending on the type of fibre. The spectrum of the LRL fibre (which is similar to this one of the LSL fibre) presents an unique peak that is lightly displaced to right. This provokes that the difference of the mean wavelength between booths sources is more less 12 nm. The reason of this behaviour is to be found in that the 1550 nm forward signal is the pump source for 1580 nm amplification band. [9]. The absorption peak and the mean wavelength for these tree fibres are shown in table 3. As can be observed, this displacement is more noticeable with high concentration fibres because the absorption peak in 1550 nm is bigger and, as a consequence, there are more emitted photons in the 1580 band.

	Comercial	LSL	LRL
1550 nm absorption peak (dB/m)	2	7	14
Mean wavelength (DPF)	1552,8 nm	1564,3 nm	1565,1 nm

Table 3. Values of absorption peak and mean wavelength of the tree fibres.

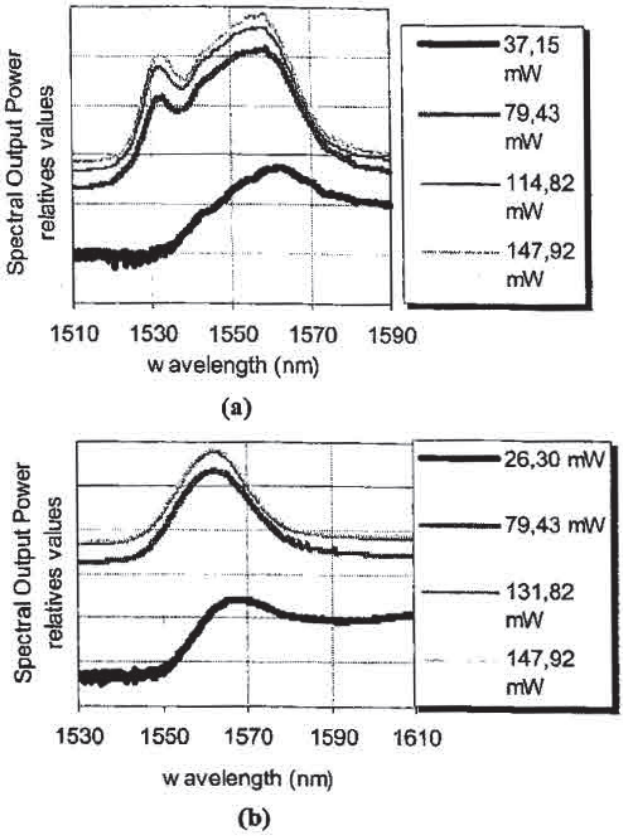

Figure 4. Evolution of the output spectrum with the pump power a) commercial fibre-DPF configuration; b) LRL fibre-DPF configuration.

The total output ASE power as a function of the pump power for different configurations is shown in figure 5. In both double pass configurations (DPB and DPF), the fiber more efficient is the LSL fiber. The difference of the efficiency between the LSL and LRL fibres is a 3.75% in the DPB configuration. The difference of the efficiency obtained from the simulation results was 2.06 %. Therefore, the experimental results are agreed with the theoretical results.

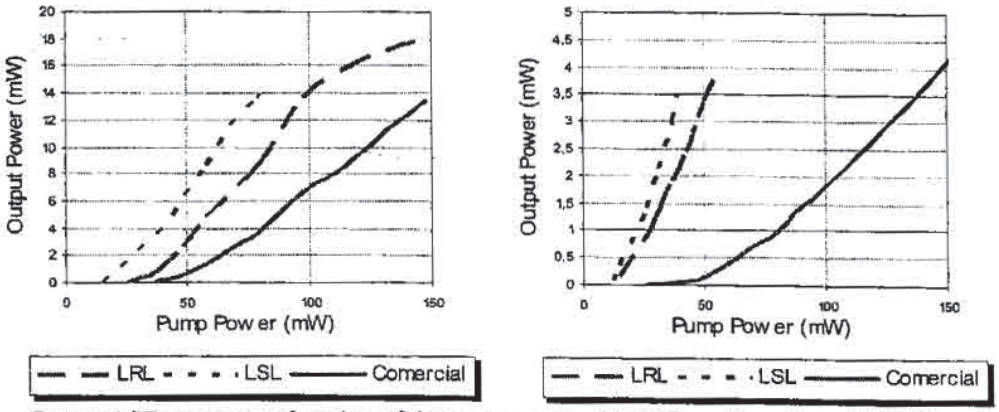

Figure 5. Output ASE power as a function of the pump power: (a) DPF configuration, (b) DPB configuration.

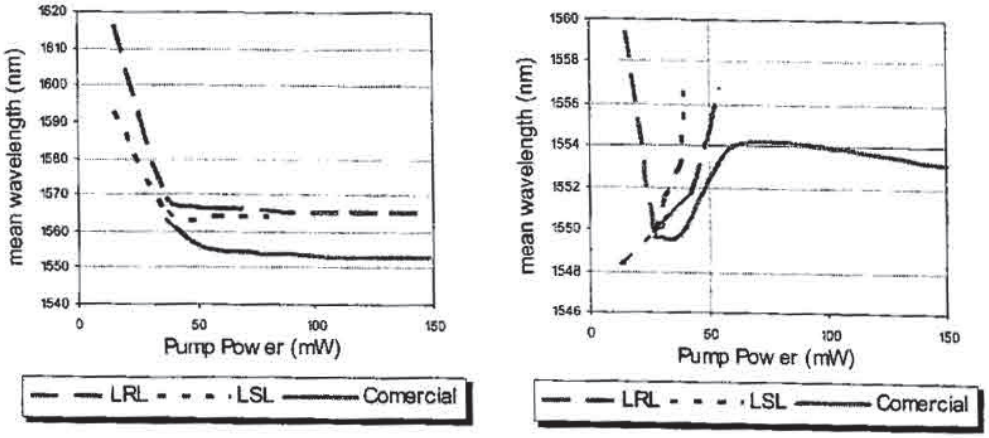

Figure 6. Mean wavelength as a function of the pump power: (a) DPF configuration, (b) DPB configuration.

Figure 6 (a) and (b) show the variation of the mean wavelength with the pump power for the DPF and DPB configurations, respectively. From these figures, it can be observed that the DPF configuration presents a bigger stability of the mean wavelength with the pump power than the DPB configuration for high pump powers. In this region of high pump powers, the two fibres more stable are the commercial and LRL fiber. For the DPB configuration, the commercial EDF has a zone of the high stability for pump powers between 67 mW and 100 mW, but the others fibres are very unstable, as can be seen in figure 6(b).

The zone of maximum stability of the DPF and DBB configurations for these three fibres coincides with the zone of maximum outpout power. Nevertheless, in this zone the spectral width is not maximum, as can be observed in figures 7. In the DPF configuration, the commercial EDF is the fiber that presents a bigger and more stable spectral width for high pump powers. In the DPB configuration, the commercial EDF is also the more optimum from the point of view of the spectral width. The LRL EDF has a bigger spectral width than the commercial EDF only for pump powers between 42 mW and 54 mW.

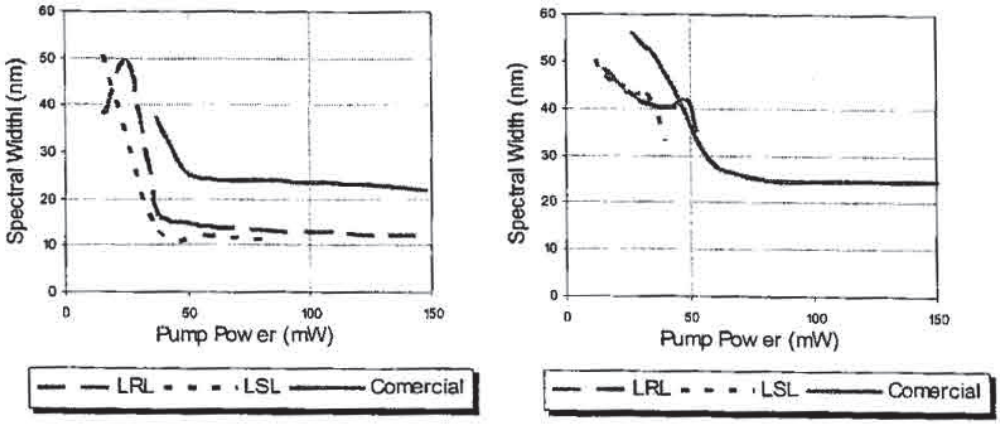

Figure 7. Spectral width as a function of the pump power: (a) DPF configuration, (b) DPB configuration

Experimental results show that the maximum pump power launched into the EDF depends on the type of fiber and the configuration. This is due to the appearance of oscillation modes from a threshold pump power. This is a highly

undesirable effect. The LSL EDF has the minor threshold pump power. On the other hand, the DPF configuration presents the bigger threshold pump power. The reason for this is to be found in that the pump and ASE signals have the same direction. This reduces unwanted reflections that provoke oscillations modes in the ASE spectrum. The output parameters more important of the DPF and DPB configurations are shown in table 4. When the threshold pump power is not indicated means that is bigger than 150 mW.

DPF					
	$P_{threshold}$ (mW)	P_{outmax} (mW)	Mean wavelength (nm)	$\Delta\lambda$ (nm)	γ(ppm/mW)
Comercial	--	13,46	1552,8	21,91	0
LRL	--	18,14	1565,1	12,01	0
LSL	85	13,85	1564,3	11,35	62,03
DPB					
	$P_{threshold}$ (mW)	Pout (mW)	Mean wavelength (nm)	$\Delta\lambda$ (nm)	γ(ppm/mW)
Comercial	--	4,00	1553,2	24,68	-12,02
LRL	52	3,749	1556,8	31	>100
LSL	42	3,522	1556,6	32,84	>>100

Table 4. Output parameters of DPF and DPB configurations. γ is the variation of the mean wavelength with the pump power.

4.1 Experimental results on the temperature dependence

To investigate the temperature dependencies of the behavior of SFS sources the EDF is isolated within a climatic chamber. The temperature is cycled from -10 to 70 °C. The configurations analyzed were: DPB with LRL EDF, DPF with LSL EDF and both configurations with commercial EDF. The election of these configurations for the LRL and LSL fibres is due to that these fibres present a similar behavior with respect to the stability wavelength independently of the configuration and, a single type of fiber has been used for each configuration. The stability of the mean wavelength with the temperature is a parameter important of these sources. Experimental results of the variation of the mean wavelength as a function of the temperature for different configurations and pump powers are shown in figure 8. From the latter it can be deduced that the variation of the mean wavelength increases with the pump power independently of the configuration.

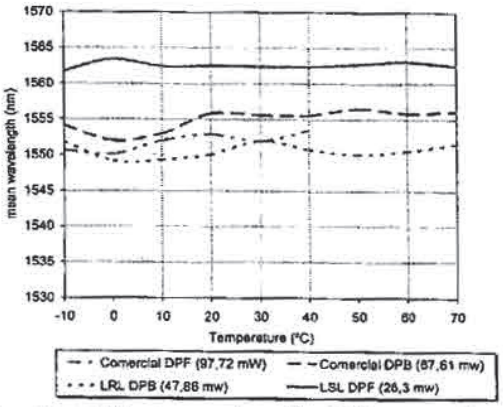

Figure 8. Mean wavelength as a function of the temperature for different configurations and pump powers: commercial-DPF and pump power=97.72 mW, commercial-DPB and pump power=67.61 mW, LRL-DPB and pump power=47.86 mW, LSL-DPF and pump power=26.3 mW..

5. CONCLUSIONS

In this paper the simulation results and experimental characterization of different SFS configurations have been presented. The theoretical model permits obtain the optimum EDF length to maximum output power. From the experimental results, it is found that the DPB configuration is the optimal to achieve a high spectral width. On the other hand, the DPF configuration offers a high efficiency and a highest stability of the mean wavelength. Moreover, this configuration is appropriate to achieve a L-band SFS source. Experimental results on the temperature dependence of the mean wavelength between -10°C and 70°C have been also reported. The variations of the mean wavelength increase with the pump power.

6. ACKNOWLEDGEMENT

This work is co-funded by the Spanish Ministry of Science and Technology through EOAMOP (TIC'2002-01259) R&D project.

REFERENCES

[1] López-Higuera José Miguel. "Superfluorescent Fiber optic Sources." Capítulo diez del libro 'Handbook of fibre sensing technology". Editado por JM López-Higuera, Wiley &Sons, Inc, pp 87-204 , July 2001.

[2] E. Desurvire, D. Bayart, B. Desthieux, S. Bigo, Erbium-doped Fiber amplifiers: Device and System Developments, Ed. Wiley & Sons, (2002).

[3] D.G. Falquier, M.J.F. Digonnet y H.J. Shaw. "A polarization-stable Er-doped superfluorescent fiber source including a Faraday rotator mirror." IEEE Photonics technology letters, Vol 12, N0 11, pp 1465-1467, 2000.

[4] D.G. Falquier, M.J.F. Digonnet y H.J. Shaw. "Improved polarization stability of the output mean wavelength in an Er-doped superfluorescent fiber source incorporating a Faraday rotator mirror." Proceedings of. SPIE Vol 3847, September 1999.

[5] Lon A. Wang y C. D. Su. "Modeling of a double-pass backward Er-doped superfluorescent fiber source for fiber.optic gyroscope applications". Journal of Lightwave Tecnology,Vol 17, pp 2307-2315,1999.

[6] K.Y. Paul, Ko y M.S. Demokan. "Temperature dependence of the amplified spontaneous emission in erbium-doped fiber amplifiers" Proceedings of the IEEE,Conference on Computer, Communication, Control and Power Engineering, pp 517-520, 1993.

[7] Paul F. Wysocki, M. J. F. Digonnet, B. Y. Kim, y H. J. Shaw. "Characteristics of Erbium-doped superfluorescent fiber sources for interferometric sensor applicationd". Journal of Lightwave technology. Vol 12, No. 3, pp 550-567, 1994.

[8] L. A Wang y C. D. Chen. "Comparison of efficiency and output power of optimal Er-doped superfluorescent fibre sources in different configurations" Electronics letters, Vol 33, No 8, pp 703-704, 1997.

[9] Shih Hsu, Tsair-Chun Liang and Yung-Kuang Chen. "Optimum Configuration and design of L-Band Erbium-Doped Supefluorescent Fiber Source." Jpa. Appl. Phys. Vol 41, pp 3724-3729, (2002).